

Radiative decay of K^-p system and photoproduction of $\Lambda(1405)$

Tae Keun Choi

Department of Physics, Yonsei University, Wonju, 220-710, Korea

Kyung Sik Kim and Byung Geel Yu*

School of Liberal Arts & Sciences, Korea Aerospace University, Koyang, 412-791, Korea

The properties of the $\Lambda(1405)$ resonance have been investigated from radiative decay of $K^-p \rightarrow Y\gamma$ and photoproduction $\gamma p \rightarrow K^+\Lambda(1405)$ within the framework of the isobar model. For a consistent result with recently measured branching ratios, the axial vector meson $K_1(1270)$ is taken into account. Strong and electromagnetic coupling constants of $\Lambda(1405)$ are extracted from these branching ratios and are applied to the analysis of $K^+\Lambda(1405)$ photoproduction. The total and differential cross sections are predicted.

PACS numbers: 23.50.+z, 23.20.-g, 14.20.jn

Keywords: Radiative decay, Branching ratio, K_1 meson, $\Lambda(1405)$ photoproduction

I. INTRODUCTION

Radiative decays $K^-p \rightarrow \Lambda\gamma$ and $K^-p \rightarrow \Sigma^0\gamma$ are important processes to study the nature of the $\Lambda(1405)$ resonance because of the proximity of the K^-p system to the mass of the subthreshold $\Lambda(1405)$ [1, 2]. From parity and angular momentum conservation, it is clear in these decay processes that the s-channel exchange of the $\Lambda(1405)$ resonance must be predominant at threshold[3, 4]. Therefore, information on the $\Lambda(1405)$ couplings can be obtained by analyzing these radiative decays.

Measurements of the branching ratio were recently renewed by the Brookhaven experiment. They were reported to be $R_{\Lambda\gamma} = (0.86 \pm 0.07^{+0.10}_{-0.08}) \times 10^{-3}$ and $R_{\Sigma^0\gamma} = (1.44 \pm 0.20^{+0.12}_{-0.10}) \times 10^{-3}$ [5]. These new measurements improved previous experimental values $R_{\Lambda\gamma} = (2.8 \pm 0.8) \times 10^{-3}$ and $R_{\Sigma^0\gamma} \leq 4 \times 10^{-3}$, which might contain attributions either from in-flight $\Lambda\pi^0$ or pile up to the $\Lambda\gamma$ and $\Sigma^0\gamma$ events with poor energy resolution[6]. On the other hand, however, theoretical estimates on these processes within the framework of the isobar model remain untouched, with old predictions for the past experimental values[7, 8].

In our previous work[9], we showed that inclusion of the t-channel exchange of the axial vector meson $K_1(1270)$ could improve the model prediction for these ratios, because the $K_1(1270)$ with spin parity 1^+ was allowed by parity and angular momentum conservation at threshold, as well as $\Lambda(1405)$. Here, we investigate the reaction process $\gamma p \rightarrow K^+\Lambda(1405)$ by using the result of our previous work to constrain the process. To be more specific, we calculate cross sections for photoproduction $\gamma p \rightarrow K^+\Lambda(1405)$ with the coupling constants

determined from the decay process of the K^-p system. Due to the scarcity of experimental data, however, this process has rarely been studied. Therefore, the numerical consequences in this work will be predictions for future experiments.

In Section I, we give a brief summary of the branching ratio $R_{Y\gamma}$ studied in Ref.[9] with emphasis on the additional contribution of K_1 exchange, and we compare the result with those of Refs.[7, 8]. In the next section, we calculate the total and differential cross sections for $\gamma p \rightarrow K^+\Lambda(1405)$. We discuss the results in the final section.

II. RADIATIVE KAON CAPTURE

The decay width for the process $K^-(q) + p(p) \rightarrow Y(p') + \gamma(k)$ is given by

$$\Gamma_{K^-p \rightarrow Y\gamma} = |\phi_K(0)|^2 \frac{M_Y |k|}{4\pi W m_K} \frac{1}{2} \sum_s \sum_{\lambda, s'} |\mathcal{M}|^2, \quad (1)$$

where q , p , p' , and k are the 4-momenta of the kaon, proton, hyperon, and photon with masses m_K , M , M_Y , respectively. The $\phi_K(0)$ is the wave function of the kaon captured at the s-orbit with respect to a proton, and W is the invariant mass of the process. The width is evaluated at threshold $(\sqrt{s}, \mathbf{0})$ in the center of mass frame with the spin-average for the initial state and the spin-sum for the final state interacting particles. Then, the branching ratio is defined as

$$R_{Y\gamma} = \frac{\Gamma_{K^-p \rightarrow Y\gamma}}{\Gamma_{K^-p \rightarrow all}}, \quad (2)$$

where $\Gamma_{K^-p \rightarrow all} = 2W_p |\phi_K(0)|^2$ is the decay width of the K^-p system for all channels and $W_p = (560 \pm 135)\text{MeV fm}^3$ is the pseudopotential of the K^-p system[7].

With the transition amplitude \mathcal{M} in Eq.(1) given in Ref.[7], the t-channel $K_1(1270)$ exchange is obtained by

*Electronic address: bgyu@kau.ac.kr

TABLE I: Coupling constants for the non-resonant Born terms and meson exchanges in the radiative decay processes $K^-p \rightarrow \Lambda\gamma$ and $\Sigma^0\gamma$. Anomalous magnetic moments are given in units of the proton magneton, $\frac{e}{2M}$, $\kappa_p = 1.793$, $\kappa_\Lambda = -0.613$, $\kappa_{\Sigma^0} = 0.619$, and $\kappa_{\Sigma^0\Lambda} = 1.60$. The coupling constants $g_{\gamma KK^*}$ and $g_{\gamma KK_1}$ are in units of GeV^{-1} . Nucleon and hyperon resonances are taken into account from Ref.[7].

| | WF | Type I | Type II |
|---|-------------|-------------------|--------------|
| $g_{Kp\Lambda}$ | -13.2 | $-13.2\sqrt{0.3}$ | -13.2 |
| $g_{Kp\Sigma^0}$ | 6.0 | $6.0\sqrt{0.3}$ | 6.0 |
| $g_{\gamma KK^*}$ | 0.254 | 0.254 | 0.254 |
| $g_{K^*p\Lambda}^V (g_{K^*p\Lambda}^T)$ | -4.5(-16.7) | -4.5(-16.7) | -4.5 (-16.7) |
| $g_{K^*p\Sigma}^V (g_{K^*p\Sigma}^T)$ | -2.6(3.2) | -2.6(3.2) | -2.6 (3.2) |
| $g_{\gamma KK_1}$ | - | - | -0.6 |
| $g_{K_1p\Lambda}^V (g_{K_1p\Lambda}^T)$ | - | - | -5.2 (-9.66) |
| $g_{K_1p\Sigma}^V (g_{K_1p\Sigma}^T)$ | - | - | -3 (1.86) |

replacing $k \rightarrow -k$ and $q \rightarrow -q$ in the photoproduction amplitude[9, 10] on the basis of crossing symmetry between the two processes. We have estimated the anomalous coupling constant $g_{\gamma KK_1}$ by applying the vector meson dominance to the strong coupling vertex ρKK_1 [11]. The strong coupling constants $g_{K_1pY}^V$, and $g_{K_1pY}^T$ can be determined by using the SU(3) octet relations[9, 12, 13].

In Table I, we list principal coupling constants for the non-resonant Born terms and the K^* and K_1 resonances couplings used for the calculation of branching ratios. On the basis of the same set of nucleon and hyperon resonances as those of Ref.[7], the WF in Table I refers to the model calculation of Ref.[7], Type I to Ref.[8], and Type II to the present work with the K_1 contribution to WF. The coupling constants of $\Lambda(1405)$ for strong and magnetic interactions, $g_{Kp\Lambda_{1405}}$, $\kappa_{\Lambda\Lambda_{1405}}$, and $\kappa_{\Sigma^0\Lambda_{1405}}$, are not known yet. For the calculation of the branching ratio, we use $g_{Kp\Lambda_{1405}} = 3.2$ (with an overall sign ambiguity), which is favored in the literature. The magnetic couplings $\kappa_{\Lambda\Lambda_{1405}}$ and $\kappa_{\Sigma^0\Lambda_{1405}}$ are treated as parameters to be determined from the experimental data.

In Fig. 1, we show the result, omitting the case of $\Sigma^0\gamma$ decay, which does not reveal the significance of the role of the K_1 because of the much smaller contribution of the non-resonant Born terms. It is clear in Fig. 1 that the WF model given by the dashed line can hardly account for the experimental value in the case of $\Lambda\gamma$ decay. As discussed in Ref.[7], the assumed value $\kappa_{\Lambda\Lambda_{1405}} \approx -0.4$ at the minimum of the dashed curve corresponds to $R_{\Lambda\gamma} = 1.22$ for the pseudoscalar (PS) coupling, and 1.14 for the pseudovector (PV) coupling scheme, neither of which is in the range of the experimental measurement. In case of the Type I model, the reduction of the coupling constants $g_{Kp\Lambda} \rightarrow \sqrt{0.3}g_{Kp\Lambda}$ on the $R_{\Lambda\gamma}$ (and $g_{Kp\Sigma^0} \rightarrow \sqrt{0.3}g_{Kp\Sigma^0}$ on the $R_{\Sigma^0\gamma}$) leads to a suppression of the Born contribution by a factor of 30%, as claimed in Ref.[8]. We find in the Type I, however, the contribution of $\Lambda(1405)$ to the $\Lambda\gamma$ decay is

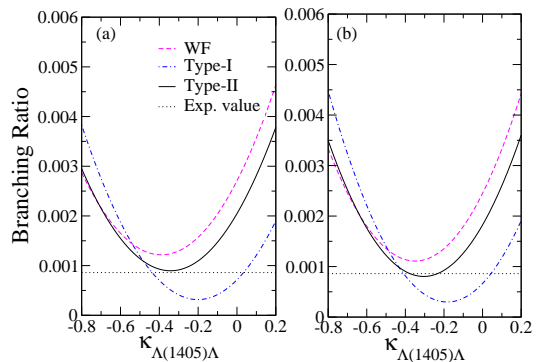


FIG. 1: The branching ratio $R_{\Lambda\gamma}$ for the $K^-p \rightarrow \Lambda\gamma$ decay process. In each panel, the dashed line is from the WF model, the dash-dotted line is from the Type I, and the solid line is from the Type II. The experimental value is denoted by the horizontal dotted line. The PS scheme is given in (a) and the PV scheme in (b).

by an order of magnitude smaller than that of the WF model, or of the Type II. Within the present framework, therefore, the dominance of $\Lambda(1405)$ in the $\Lambda\gamma$ decay cannot be supported by the Type I model. The Type II model exhibits the contribution of K_1 meson to the $R_{\Lambda\gamma}$ with coupling constants given in Table I. These are presented as the solid lines in Fig. 1. The solid line in Fig. 1(a) has an intersection at $\kappa_{\Lambda\Lambda_{1405}} = -0.34$ to estimate $R_{\Lambda\gamma} = 0.9$ in the PS scheme while it yields a set of value for $\kappa_{\Lambda\Lambda_{1405}} = (-0.38, -0.23)$, consistent with $R_{\Lambda\gamma} = 0.86$ for the PV scheme in Fig. 1(b). As shown, the deviation of the solid line from the dashed one due to the K_1 contribution is significant enough to give $\kappa_{\Lambda\Lambda_{1405}}$ a physical value.

III. $K^+\Lambda(1405)$ PHOTOPRODUCTION

In this section, we investigate photoproduction $\gamma p \rightarrow K^+\Lambda(1405)$ within the same framework of the previous section. We restrict our aim here to a report of the numerical result from the qualitative viewpoint, because experimental data are very scarce for a direct comparison.

With the convention for 4-momenta,

$$\gamma(k) + p(p) \rightarrow K^+(q) + \Lambda_{1405}(p'), \quad (3)$$

the cross section is given by

$$\frac{d\sigma}{d\Omega} = \frac{MM_{\Lambda_{1405}}}{16\pi^2 W^2} \frac{|q|}{|\mathbf{k}|} \frac{1}{4} \sum_{\lambda_\gamma, s, s'} |\mathcal{M}|^2. \quad (4)$$

The transition amplitude \mathcal{M} for the photoproduction of the negative parity $\Lambda(1405)$ is obtained by replacing $\bar{u}_\Lambda(p_\Lambda)\gamma_5 \rightarrow -\bar{u}_{\Lambda_{1405}}(p')$ in the $\gamma p \rightarrow K^+\Lambda$ photoproduction given in Ref.[10]. For consistency, we use the pseudoscalar coupling constants given in the previous section

TABLE II: Coupling constants taken from the radiative decay process $K^-p \rightarrow Y\gamma^a$ [7] and photoproduction, $\gamma p \rightarrow K^+\Lambda(1405)^b$ [16]. Values for the present work^c are taken from Ref.[9]. Anomalous magnetic moments are given in units of the proton magneton $\frac{e}{2M}$. $G_{K^*}^V = g_{\gamma KK^*}g_{K^*p\Lambda 1405}^V$, and $G_{K_1}^V = g_{\gamma KK_1}g_{K_1p\Lambda 1405}^V$.

| | WF ^a | WJC ^b | present work ^c |
|--------------------------------|-----------------|------------------|---------------------------|
| $g_{Kp\Lambda}$ | -13.2 | 4.127 | -13.2 |
| $g_{Kp\Sigma^0}$ | 6 | -0.329 | 6 |
| $g_{Kp\Lambda 1405}$ | 3.2 | 1.5 ~ 3.0 | 0.9 ~ 3.2 |
| $\kappa_{\Lambda 1405}$ | - | 0.44 | -0.44 |
| $\kappa_{\Lambda\Lambda 1405}$ | ≈ -0.4 | -0.224 | -0.34 |
| $\kappa_{\Sigma\Lambda 1405}$ | -0.26 | 1.077 | -0.23 |
| $g_{KN_{1710}\Lambda 1405}$ | 0.81 | 0.81 | 0.81 |
| $g_{KN_{1650}\Lambda 1405}$ | 6.5 | 6.4 | 6.5 |
| $\kappa_{N_{1710}p}$ | 0.03 | 0.097 | 0.03 |
| $\kappa_{N_{1650}p}$ | 0.32 | -0.41 | -0.32 |
| $G_{K^*}^V$ | - | - | 0.276 |
| $G_{K_1}^V$ | - | - | 0.395 |

to calculate the cross sections. Since the reaction channel opens almost $W = 1.9$ GeV above, we assume that the roles of baryon resonances will not be significant because fewer resonances with masses around 2 GeV are reported. For comparison with existing calculations, we consider $N^*(1650)\frac{1}{2}^-$ and $N^*(1710)\frac{1}{2}^+$ for the s-channel, and $\Lambda(1405)\frac{1}{2}^-$ for the u-channel exchanges. The couplings of $\Lambda(1405)$ to the vector mesons K^* and K_1 are currently not known. We utilize the ratio $\frac{G_{K^*}^V}{G_{K_1}^V} \simeq -0.7$ extracted from the WJC model fitted to the K^+Y electroproduction data[14]. Resuming the ratio, we give the values for the couplings shown in Table II at this exploratory stage, with assumptions that these values be less than $g_{Kp\Lambda 1405}$ and that the cross section be less than that of $K^+\Lambda$ photoproduction[15]. We here neglect the tensor couplings of these vector mesons for the minimal model calculation.

In Table II, we list the coupling constants of the present work and compare them with those used for the decay width[7] and for the photoproduction[16] in other model calculations. The values of the WJC model are taken from Ref.[16]. In this model, meson exchanges in the t-channel are not considered by the duality between s- and t-channel. Thus, not only the K^* but the K_1 exchange is absent from the model. Note that the WF values in Table II for the K^* and the K_1 coupling constants are irrelevant here because they are, now, coupling to the $\Lambda(1405)$. We must address that, while there is ambiguity in the sign of $g_{Kp\Lambda 1405}$, we choose the sign of the $\kappa_{\Lambda 1405}$ to be opposite to the WJC one, as in Table II, in consideration of the relative signs between $g_{Kp\Lambda 1405}$ and $\kappa_{\Lambda 1405}$ in Ref.[14]. We also take the sign of the coupling constant $\kappa_{N_{1650}p}$ of WJC to be opposite to the original one in Ref.[16] in order for

the cross section to decrease beyond the resonance region, $E_\gamma \approx 2$ GeV. With the cutoff Λ for the hadron form factors taken as 1.2 GeV for the non-resonant Born terms and 1.8 GeV for the resonances[10], the numerical results are presented in Fig. 2 for the total cross section and in Fig. 3 for the differential cross section, respectively.

IV. RESULTS AND DISCUSSION

In Fig. 2, dashed and dash-dotted curves are the cross sections of the model with WJC coupling constants taken, each of which results from varying $g_{Kp\Lambda 1405}$ from 1.5 to 3.0, respectively. The result of the present work is shown in the dash-dot-dotted, dotted, and solid lines corresponding to the choice of $g_{Kp\Lambda 1405} = 0.9, 1.5,$ and 3.2 in order. It should be noted that all the curves in Figs. 2 and 3 are calculated with the use of the same form factors in both models, i.e., the model with WJC values and the present work for comparison, although the former in Ref.[16] does not consider such form factors. In the absence of these form factors, however, the maximum height of the WJC cross section becomes by an order of magnitude larger than the present one. As shown in this figure, the cross section is very sensitive to changes in the leading coupling constant $g_{Kp\Lambda 1405}$.

Figure. 3 shows the angular distributions in both model calculations near threshold, $E_\gamma = 1.6$ GeV. The solid curve results from the present work, and the dotted one from the model with WJC values, where $g_{Kp\Lambda 1405} = 3.0$ is taken in common for comparison. The angular distribution of the former represents an apparent feature of p-wave production, indicating a rapid increase of the t-channel kaon exchange[17], while the latter demonstrates the backward increase implementing the strong u-channel contribution, which in the present study might be due to the hyperon exchanges considered. In fact, such a distinction can be thought of as a natural consequence of the different choice of coupling-channels; i.e., the absence of t-channel couplings from the model with WJC values leads to the u-channel enhancement.

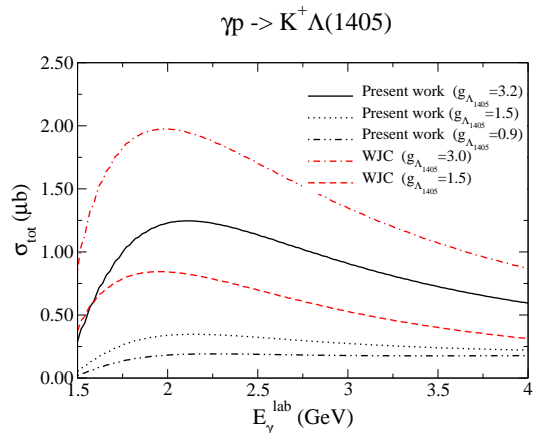


FIG. 2: Total cross section for the $\gamma p \rightarrow K^+\Lambda(1405)$ process.

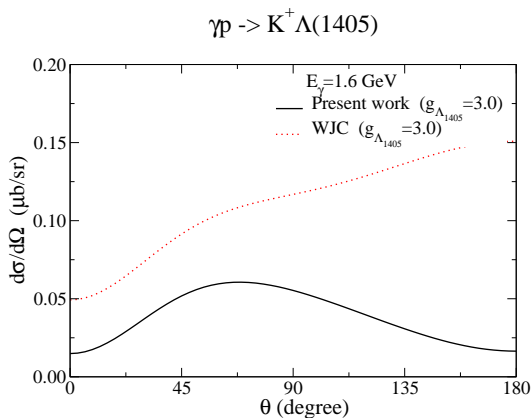


FIG. 3: Differential cross section near threshold $E_\gamma = 1.6$ GeV.

In this work, we have presented an analysis of the branching ratio of $K^-p \rightarrow Y\gamma$ and have applied the obtained coupling constants to an analysis of the $\gamma p \rightarrow K^+\Lambda(1405)$ process in the framework of the isobar model. Introducing the axial vector meson $K_1(1270)$ from parity and angular momentum conservation, we have improved the model prediction for the branching ratio. Related to this issue, we make a comment on the unitary coupled channel approach to these processes, in which the role of the initial state interaction in the $K^-p \rightarrow \Lambda\gamma$ process is emphasized[18]. In this model, the resonance state $\Lambda(1405)$ is generated in a noble way such as the quasi-bound state of a $\bar{K}N$ or a $\pi\Sigma$ coupled channel[18, 19]. We note in Ref.[18], however, that such an approach to the radiative decay of the K^-p system yields an overes-

timate of the branching ratio, which amounts to double the value of the measured one for the $\Lambda\gamma$ decay; i.e., $R_{\Lambda\gamma} = 1.58$ (without cut-off Λ_π). Thus, it needs further corrections, apart from the model dependence due to the cutoff Λ_π .

We have investigated the photoproduction $\gamma p \rightarrow K^+\Lambda(1405)$ with relevant coupling constants constrained from the radiative decay of the K^-p system. Cross sections are reproduced for our further understanding of the strong and the electromagnetic properties of the $\Lambda(1405)$ through the production mechanism. We found in this work that the magnitude of the cross section for the $K^+\Lambda(1405)$ photoproduction was of an order of micro barn, which was very sensitive to variations in the leading coupling constant $g_{Kp\Lambda 405}$. Without resonances with masses around 2 GeV near threshold, large sensitivity of the cross section to the change of $g_{Kp\Lambda 405}$ could be a useful tool for determining the coupling constant by measuring cross sections in future experiments. As discussed, the difference between the angular distributions reproduced in both models is contrasting. They reveal the respective features of the t-channel and the u-channel contributions, which are to be distinguished, as well, from future experiments.

Acknowledgments

This work was supported by the Korea Research Foundation (KRF) Grant funded by the Korean government (KRF-2008-313-C00205), and by the Korea Science and Engineering Foundation (KOSEF) Grant funded by the Korea government(MOST)(R01-2007-000-20569-0).

-
- [1] J. W. Darewych, M. Horbatsch, and R. Koniuk, Phys. Rev. D **28**, 1125 (1983).
 - [2] E. A. Veit, B. K. Jennings, R. C. Barrett, and A. W. Thomas, Phys. Lett. B **137**, 415 (1984).
 - [3] J. W. Darewych, R. Koniuk, and N. Isgur, Phys. Rev. D **32**, 1765 (1986).
 - [4] Y. S. Zhong, A. W. Thomas, B. K. Jennings, and R. C. Barrett, Phys. Lett. B **171**, 471 (1986).
 - [5] D. A. Whitehouse, *et al.*, Phys. Rev. Lett. **63**, 1352 (1989).
 - [6] J. Lowe, *et al.*, Nucl. Phys. B **209**, 16 (1982).
 - [7] R. L. Workman and Harold W. Fearing, Phys. Rev. D **37**, 3117 (1988).
 - [8] H. Burkhardt and J. Lowe, Phys. Rev C **44**, 607 (1991).
 - [9] Byung Geel Yu, and Tae Keun Choi, J. Korean Phys. Soc. **51**, L1867 (2007).
 - [10] Byung Geel Yu, J. Korean Phys. Soc. **48**, L178 (2006).
 - [11] K. Haglin, Phys. Rev. C **50**, 1688 (1994).
 - [12] J. W. Durso, and G. E. Brown, Nucl. Phys. A **430**, 653 (1984).
 - [13] L. Gamberg, and G. R. Goldstein, hep-ph/0106178.
 - [14] R. A. Williams, Chueng-Ryong Ji, and S. R. Cotanch, Phys. Rev C **46**, 1617 (1992).
 - [15] Seung-il Nam, Ji-Hyoung Park, Atsushi Hosaka, and Hyun-Chul Kim, hep-ph/0806.4029.
 - [16] R. A. Williams, Chueng-Ryong Ji, and S. R. Cotanch, Phys. Rev C **43**, 452 (1991).
 - [17] Byung-Geel Yu, Tae-Keun Choi, and Chueng-Ryong Ji, Phys. Rev. C **70**, 045205 (2004); J. Phys. G **32**, 387 (2006).
 - [18] T.-S. H. Lee, J. A. Oller, E. Oset, and A. Ramos, Nucl. Phys. A **643**, 402 (1998).
 - [19] J. K. Ahn, J. Korean Phys. Soc. **43**, S14 (2003).